Acta Crystallographica Section A
Foundations of Crystallography
ISSN 0108-7673

Received 6 June 2012
Accepted 28 October 2012

Bent perfect crystals as X-ray focusing polychromators in symmetric Laue geometry

J.-P. Guigay,[a]* C. Ferrero,[a] D. Bhattacharyya,[b] O. Mathon[a] and S. Pascarelli[a]

[a]European Synchrotron Radiation Facility, BP 220, 38043 Grenoble cedex, France, and [b]Spectroscopy Division, Bhabha Atomic Research Centre, Mumbai 400094, India. Correspondence e-mail: guigay@esrf.fr

The focusing properties of cylindrically bent crystals in symmetric Laue geometry are discussed using the formalism of Fresnel diffraction and the analytical solution of the Takagi–Taupin equations for a point source on the entrance surface. The existence of a focal shift in the dynamical focusing effect is pointed out and discussed. The present theoretical framework is applied to experiments performed at the energy-dispersive X-ray absorption spectroscopy beamline of the European Synchrotron Radiation Facility concerning the position and the size of the focal spot obtained from a polychromatic source at a large distance from the bent crystal.

1. Introduction

Bent crystal plates in Laue geometry are frequently used at synchrotron beamlines as focusing elements, forming a demagnified image of a distant source. The present theoretical framework was developed for the symmetric Laue case with the purpose of comparing theoretical predictions with experimental results obtained by some of the authors (D. Bhattacharyya, O. Mathon and S. Pascarelli).

Rays of different energies coming out of a point source and in exact Bragg incidence on a flat crystal in transmission geometry converge downstream of it in the point symmetric to the source with respect to the crystal mid-plane. In the case of a cylindrically bent crystal, this 'polychromatic focusing' effect, which does not depend to a first approximation on the crystal thickness, occurs under the condition (Chukhovskii & Krisch, 1992)

$$\frac{1}{q}-\frac{1}{p}=\frac{2}{R\cos\theta_{\rm B}}, \qquad (1)$$

where p is the source-to-crystal distance, q is the crystal-to-focus distance, $\theta_{\rm B}$ is the Bragg angle and R is the radius of curvature of the crystal, which is taken as positive in the present investigation, that is to say the source faces the convex side of the crystal. In the design of an energy-dispersive X-ray absorption spectroscopy beamline, one uses a position-sensitive detector downstream of a sample placed in the focal position. In this way, the absorption spectrum of the sample can be recorded over the whole energy range of the reflected beam (Hagelstein *et al.*, 1995).

The optical performance of such a crystal (polychromator), in particular the size of the focal spot, depends on the crystal thickness *via* the 'dynamical focusing' effect, which was described decades ago by Afanasev & Kohn (1977) and Aristov *et al.* (1978, 1980) in the flat crystal case, and by Kushnir & Suvorov (1982) in the bent crystal case; see also the book by Pinsker (1978). According to Mocella *et al.* (2004, 2008), the focal size should be minimized when the dynamical and polychromatic foci are made to coincide by the choice of the crystal thickness (see also Sanchez del Rio *et al.*, 1994).

A novel aspect of the theory of dynamical focusing is reported in the present study and regards a theoretical framework explaining a non-negligible displacement of the focus position (focal shift) as well as the influence of anomalous absorption; this is briefly presented in the flat crystal case for the sake of clarity in §2. Our main contribution is, however, to show that the wavefunction downwards from a bent crystal is not obtained by successive convolutions, owing to the analytical form of the phase factor by which the propagator of a bent crystal differs from that of the flat crystal case. This finding has lead us not to use the Fourier transform formalism which is convenient for flat crystals, as shown for instance by Kohn *et al.* (2000).

The calculations are instead carried out following the geometric scheme depicted in Fig. 1. Let us consider a monochromatic point source S and let O be the point of the crystal entrance surface such that SO is a ray in exact Bragg incidence, and let Ω be the point at the crystal exit surface of this ray. With λ being the wavelength and SO = p, the incident amplitude along the axis Oτ perpendicular to SO is

$$D_{\rm inc}(\tau)=\exp(i\pi\tau^2/\lambda p)/(i\lambda p)^{1/2}, \qquad (2)$$

which becomes a delta function $\delta(\tau)$ as $p\rightarrow 0$ (point source on the crystal surface). The crystal propagator is expressed in such a form as to obtain the Bragg-reflected amplitude $D(u)$ along the axis Ωu perpendicular to the Bragg direction Ωq; the reflected amplitude at any point downstream from the crystal can be then calculated by a Fresnel diffraction integral.

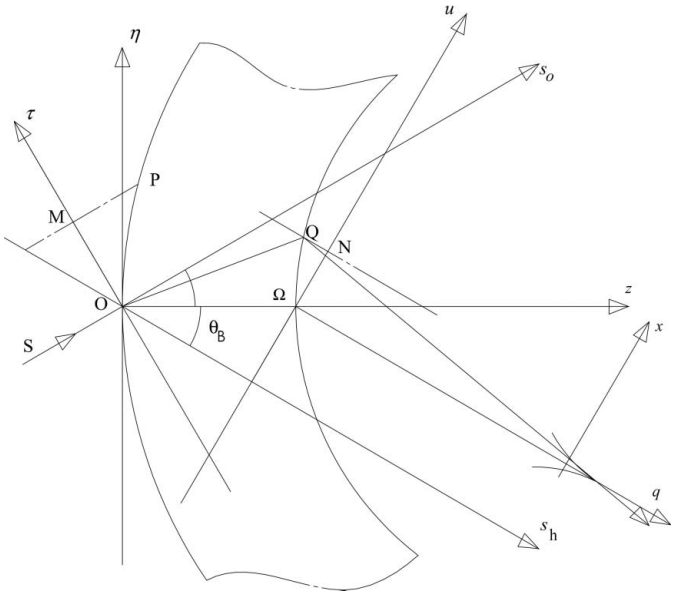

Figure 1
Illustration of the optical setup under consideration, showing the different systems of coordinates used in the text. The Oτ axis is perpendicular to Os_o; the Ωu axis is perpendicular to Ωq and to Os_h. The shape of the caustic curve is schematically shown on the right-hand side.

2. The displacement of the dynamical focus and the influence of anomalous absorption

Let us initially consider the case of a point source on the entrance surface of a flat crystal. The reflected amplitude $D(u)$ along the axis Ωu in vacuum is obtained by setting $s_{o,h} = t(a \pm u)/2a\cos\theta_B$ in the function $J_o[k(\chi_h\chi_{\bar{h}}s_o s_h)^{1/2}]$; $k = 2\pi/\lambda$; $s_{o,h}$ are oblique coordinates along the incident and Bragg directions, respectively, with a common origin in O; $\chi_{h,\bar{h}}$ are the Fourier coefficients of the crystal susceptibility; t is the crystal thickness; and $a = t\sin\theta_B$ is the half-width of the reflected beam (see Fig. 1). The Bessel function argument becomes then $Z(a^2-u^2)^{1/2}$, with $Z = k(\chi_h\chi_{\bar{h}})^{1/2}/\sin 2\theta_B$, the real part of Z being chosen as positive: $\mathrm{Re}\,Z = Z_{re} > 0$. For $|u| \ll a$ and $|Za| \gg 1$, by using the asymptotic expression

$$D(u) \simeq [2\pi Z(a^2-u^2)^{1/2}]^{-1/2}\{\exp[iZ(a^2-u^2)^{1/2} - i(\pi/4)] + \exp[-iZ(a^2-u^2)^{1/2} + i(\pi/4)]\} \quad (3)$$

and also $(a^2-u^2)^{1/2} \simeq a - u^2/2a$, one obtains

$$D(u) \simeq (2\pi iZa)^{-1/2}\left[\exp\left(iZa - i\frac{Zu^2}{2a}\right) + i\exp\left(-iZa + i\frac{Zu^2}{2a}\right)\right]. \quad (4)$$

The phase terms $\exp(\pm iZ_{re}u^2/2a)$ are the transmission functions of cylindrical lenses, convergent with the '−' sign or divergent with the '+' sign (see *e.g.* Goodman, 1968), with paraxial focal distance

$$q_0 = \frac{\pi}{\lambda}\frac{2a}{Z_{re}} = \frac{a\sin 2\theta_B}{\mathrm{Re}(\chi_h\chi_{\bar{h}})^{1/2}}. \quad (5)$$

Expression (5) is well known and is generally obtained by using a series expansion of the spherical wave in plane waves (Kohn *et al.*, 2000).

We are mainly interested in the convergent term, which is the first one in equations (3) and (4). According to equation (3), the corresponding phase modulation is

$$\varphi(u) = Z_{re}(a^2-u^2)^{1/2} \simeq Z_{re}\left(a - \frac{u^2}{2a} - \frac{u^4}{8a^3} + \ldots\right).$$

This phase modulation is responsible for the u-dependent angular deviation:

$$\theta(u) = \frac{\lambda}{2\pi}\frac{\mathrm{d}\varphi}{\mathrm{d}u} = -\frac{u}{q_0}\left(1 + \frac{u^2}{2a^2} + \ldots\right),$$

the modulus of which is larger than $|u/q_0|$. The rays around $u = 0$ cut Ωq at distances shorter than q_0 and are tangential to the caustic curve shown schematically in Fig. 1, its cusp being the paraxial focus at the distance q_0; this is indeed a cylindrical aberration effect. The point of maximum intensity along the optical axis Ωq, considered as the 'effective focus', is expected to be at an 'effective focal distance' αq_0, with $0 < \alpha < 1$. Numerical calculations of the intensity distribution along the optical axis Ωq, according to the integral expression

$$I(q) = \frac{1}{\lambda q}\left|\int_{-a}^{a}\mathrm{d}u\exp\left(\frac{i\pi u^2}{\lambda q}\right)J_0[Z(a^2-u^2)^{1/2}]\right|^2,$$

allow the determination of the parameter α, which is a function of the complex parameter $aZ = \pi t(\chi_h\chi_{\bar{h}})^{1/2}/\lambda\cos\theta_B$. In the case of a non-absorbing crystal, aZ is real and equal to $\pi t/\Lambda_0$, where Λ_0 is the *Pendellösung* distance. We have found numerically that α increases from $\alpha \simeq 0.60$ for $aZ = 10$ to $\alpha \simeq 0.80$ for $aZ = 40$. The focusing condition can be written as $q = \pm\alpha q_0$ in order to include the virtual focus corresponding to the divergent term of equation (4).

Formula (4) also gives the opportunity to discuss the influence of anomalous absorption (Borrmann effect) in a new and straightforward manner. Clearly, due to the phase term $\exp(\pm iZa)$, if the real and imaginary parts of Z are positive, the modulus of the convergent term in equation (4) is decreased, whereas that of the divergent term is increased. This is an unfavourable condition for achieving a good focusing of the reflected wave. A favourable condition would be instead $\mathrm{Re}\,Z > 0$ and $\mathrm{Im}\,Z < 0$ for the first term in equation (4) or $\mathrm{Re}\,Z < 0$ and $\mathrm{Im}\,Z > 0$ for the second term in equation (4), namely that the real and the imaginary parts of $(\chi_h\chi_{\bar{h}})^{1/2}$ should have different signs. This condition can be most simply formulated as $\mathrm{Im}\,(\chi_h\chi_{\bar{h}}) < 0$.

One can write $\mathrm{Im}\,\chi_h\chi_{\bar{h}} = 2|\chi_{rh}||\chi_{ih}|\cos(\varphi_{rh} - \varphi_{ih})$, where χ_{rh} and χ_{ih} are, respectively, the Fourier coefficients of the real and imaginary parts of the complex susceptibility and are written in the form $\chi_{rh} = |\chi_{rh}|\exp(i\varphi_{rh})$ and $\chi_{ih} = |\chi_{ih}|\exp(i\varphi_{ih})$. In the case of a centrosymmetric crystal, the cosine term is equal to ± 1 and is always equal to 1 for a monoatomic crystal. A counterexample would be the 222 reflection of calcite, $CaCO_3$ (Authier, 2005). It would be interesting to

investigate experimentally the dynamical focusing effect in such a case, *i.e.* under conditions of strong anomalous absorption.

3. The crystal propagator derived from the Takagi–Taupin equations

Let us use two mutually orthogonal axes (Oη, Oz) tangential and normal, respectively, to the crystal surface. The diffraction vector of modulus $h = 2k\sin\theta_B$ is antiparallel to Oη, as shown in Fig. 1. Upon bending, the length of the neutral surface of radius R is not changed, whereas the lengths of the entrance and exit surfaces are multiplied respectively by $(1 \pm t/2R)$. The component of the lattice displacement along Oη is $U(\eta, z) = \eta(t - 2z)/2R$. In terms of the oblique coordinates $s_{o,h} = (z\sin\theta_B \pm \eta\cos\theta_B)/\sin 2\theta_B$ we obtain

$$\mathbf{h}\cdot\mathbf{U}(\eta, z) = \eta\frac{2z - t}{R}k\sin\theta_B = \varphi(s_o) - \varphi(s_h)$$

with

$$\varphi(s_{o,h}) = \frac{k\sin\theta_B}{R}s_{o,h}(s_{o,h}\sin 2\theta_B - t\sin\theta_B). \qquad (6)$$

Using the notation $\mathbf{r}$ for the position vector of an arbitrary point in the crystal, the total wavefield can be expressed as $\exp(i\mathbf{k}_o\cdot\mathbf{r})[D_o(s_o, s_h) + \exp(i\mathbf{h}\cdot\mathbf{r})D_h(s_o, s_h)]$, $\mathbf{k}_o$ being the vacuum wavevector parallel to Os_o. The amplitudes $D_{o,h}(s_o, s_h)$ are solutions of the Takagi–Taupin equations (TTEs) (Takagi, 1962, 1969; Taupin, 1964, 1967)

$$\begin{aligned}\frac{\lambda}{\pi}\frac{\partial D_o}{\partial s_o} &= i\chi_0 D_o(s_o, s_h) + i\chi_{\bar{h}}D_h(s_o, s_h)\exp[i\varphi(s_o) - i\varphi(s_h)],\\ \frac{\lambda}{\pi}\frac{\partial D_h}{\partial s_h} &= i\chi_0 D_h(s_o, s_h) + i\chi_h D_o(s_o, s_h)\exp[i\varphi(s_h) - i\varphi(s_o)].\end{aligned} \qquad (7)$$

The incident wave is written as $\exp(i\mathbf{k}_o\cdot\mathbf{r})D_{inc}(s_o, s_h)$. Equations (7) reduce to the TTEs for a flat crystal by using

$$\begin{aligned}E_o(s_o, s_h) &= D_o(s_o, s_h)\exp[i\varphi(s_h)],\\ E_h(s_o, s_h) &= D_h(s_o, s_h)\exp[i\varphi(s_o)],\end{aligned}$$

the incident amplitude transforming into $E_{inc}(s_o, s_h) = D_{inc}(s_o, s_h)\exp[i\varphi(s_h)]$.

In the case of a point source in O on the crystal entrance surface, $D_{inc}(s_o, s_h)$ and $E_{inc}(s_o, s_h)$ are both equal to the delta function $\delta(s_h)$ and $E_h(s_o, s_h)$ reduces to the well known expression for the flat crystal case (Kato, 1961; Pinsker, 1978; Authier, 2005). This means that

$$\begin{aligned}D_h(s_o, s_h) &= \frac{i\pi\chi_h}{\lambda}J_o\left[k(\chi_h\chi_{\bar{h}}s_o s_h)^{1/2}\right]\\ &\quad\times\exp\left[i\frac{\pi}{\lambda}\chi_0(s_o + s_h) - i\varphi(s_o)\right].\end{aligned} \qquad (8)$$

In the more general case of a distant source, corresponding to a distribution of coherent elementary point sources on the entrance surface, we need the analytical form of $D_h(s_o, s_h)$ for a point source on the entrance surface such that its oblique coordinates (σ_o, σ_h) are not equal to 0. We then set $D_{inc}(s_o, s_h) = \delta(s_h - \sigma_h)$ and consequently $E_{inc}(s_o, s_h) = \delta(s_h - \sigma_h)\exp[i\varphi(\sigma_h)]$. We thus obtain

$$\begin{aligned}D_h(s_o, s_h) &= E_h(s_o, s_h)\exp[-i\varphi(s_o)]\\ &= \frac{i\pi\chi_h}{\lambda}J_0\left[k(\chi_h\chi_{\bar{h}}s'_o s'_h)^{1/2}\right]\\ &\quad\times\exp\left[i\frac{\pi\chi_0}{\lambda}(s'_o + s'_h) + i\varphi(\sigma_h) - i\varphi(s_o)\right],\end{aligned} \qquad (9)$$

where the notation $s'_{o,h} = s_{o,h} - \sigma_{o,h}$ is used. Relations (8) and (9) are used in the next section to obtain the crystal propagator linking the reflected amplitude $D(u)$ along the Ωu axis with the incident amplitude $D_{inc}(\tau)$ along the Oτ axis; we shall omit the factor $(i\pi\chi_h/\lambda)\exp[i\pi\chi_0(s'_o + s'_h)/\lambda]$, which is a constant for a crystal plate of uniform thickness.

4. Dynamical focusing by a cylindrically bent crystal

4.1. Point source on the entrance surface

Consider the points N and Q on the same line parallel to Os_h, N being on the axis Ou, Q on the curved exit surface (see Fig. 1). These points have the same coordinate $s_o = (a + u)/\sin 2\theta_B$, where u denotes the position of N on the axis Ωu. It is convenient to write the product $[s_o s_h]_Q$ as a polynomial function of degree 2 in u. The point Q being the intersection of the crystal boundary curve $z = t + \eta^2/2R\cos\theta_B$ by the straight line $z\sin\theta_B + \eta\cos\theta_B = a + u$, we can calculate the rectangular coordinates

$$\begin{aligned}[\eta]_Q &= \frac{u}{\cos\theta_B} - \frac{u^2\sin\theta_B}{2R\cos^3\theta_B} + \ldots \text{ and}\\ [z]_Q &= t + \frac{u^2}{2R\cos^2\theta_B} + \ldots\end{aligned}$$

and consequently the oblique coordinates

$$\begin{aligned}[s_o]_Q &= \frac{a + u}{\sin 2\theta_B} \text{ and}\\ [s_h]_Q &= \left(a - u + \frac{u^2\sin\theta_B}{R\cos^2\theta_B} + \ldots\right)(\sin 2\theta_B)^{-1}.\end{aligned}$$

Hence

$$\begin{aligned}[s_o s_h]_Q &= \frac{a + u}{\sin 2\theta_B}\left[\frac{a - u}{\sin 2\theta_B} + \frac{u^2}{2R\cos^3\theta_B}\right]\\ &\simeq \frac{a^2 - u^2 + u^2(a\tan\theta_B)/(R\cos\theta_B)}{\sin^2 2\theta_B}.\end{aligned}$$

The last term in the numerator can be neglected since $a\tan\theta_B \ll R\cos\theta_B$. This approximation indicates that the effects of the curvature of the exit surface are negligibly small in the calculation of $[s_o s_h]_Q$.

Formula (6) shows that $[\varphi(s_o)]_Q \simeq \pi u(a + u)/\lambda R\cos\theta_B$, then, according to equation (8), the reflected amplitude along the axis Ωu is

$$D(u) = D_h(s_o s_h)_Q = J_0[Z(a^2 - u^2)^{1/2}]\exp\left[-i\frac{\pi u(a + u)}{\lambda R\cos\theta_B}\right]. \qquad (10)$$

The linear phase term $\exp(-i\pi ua/\lambda R\cos\theta_B)$ accounts for the uniform angular deviation $\Delta\theta = a/2R\cos\theta_B$ of the reflected beam. The focusing condition

$$\frac{1}{q} - \frac{1}{R\cos\theta_B} = \pm\frac{1}{\alpha q_0} \tag{11}$$

is derived by the same approach used in §2, by taking into account the additional phase term $\exp(-i\pi u^2/\lambda R\cos\theta_B)$. It should be noted that α does not depend on the crystal curvature. A real focus is obtained if the value of q as given by equation (11) is positive. Since q_0 [see equation (5)] and $R\cos\theta_B$ are both positive, we obtain:

(*a*) If $R\cos\theta_B > \alpha q_0$, there is one real focus at a distance $q_1 = \alpha q_0 R\cos\theta_B(\alpha q_0 + R\cos\theta_B)^{-1}$.

(*b*) If $R\cos\theta_B < \alpha q_0$, there are two real foci at distances $q_{1,2} = \alpha q_0 R\cos\theta_B(\alpha q_0 \pm R\cos\theta_B)^{-1}$.

This is similar to the results obtained by Kushnir & Suvorov (1982).

4.2. Distant point source

For a point M on the Oτ axis and the point P on the curved entrance surface, with MP parallel to SO, one can easily find $[s_h]_M = [s_h]_P = -\tau/\sin 2\theta_B$, where τ denotes the position of the point M on the axis Oτ (see Fig. 1). Using equation (6), we obtain $[\varphi(s_h)]_{M,P} - [\varphi(s_o)]_{N,Q} = (\pi/\lambda R\cos\theta_B)[\tau(\tau+a) - u(u+a)]$. Bearing in mind equation (2) for the incident amplitude, the reflected amplitude along the Ωu axis is the integral expression

$$D(u) = \int_{u-a}^{u+a} \frac{d\tau}{(i\lambda p)^{1/2}} \exp\left(\frac{i\pi\tau^2}{\lambda p}\right) \exp\left[i\pi\frac{\tau(\tau+a) - u(u+a)}{\lambda R\cos\theta_B}\right] \times J_0\left\{Z[a^2 - (u-\tau)^2]^{1/2}\right\},$$

where the product of the two last factors in the integrand is the crystal propagator. We point out that this is not a function of the difference $(u-\tau)$ only; in other words, this propagator is not space-invariant; the propagation through the bent crystal is *not* a convolution, in contrast to the propagation through a flat crystal. This can be understood physically by regarding the fact that if the incident monochromatic wave is a plane one, the Bragg-reflected wave is not a plane wave, because the departure from the Bragg condition varies continuously along the entrance surface of the bent crystal.

Using the integration variable $v = u - \tau$ and introducing the definition $p_e^{-1} = p^{-1} + (R\cos\theta_B)^{-1}$, we obtain

$$D(u) = \exp\left[\frac{-i\pi u^2}{\lambda R\cos\theta_B}\right] \int_{-a}^{a} \frac{dv}{(i\lambda p)^{1/2}} \exp\left[\frac{i\pi(u-v)^2}{\lambda p_e} - \frac{i\pi av}{\lambda R\cos\theta_B}\right] J_0\left[Z(a^2 - v^2)^{1/2}\right]. \tag{12}$$

We also define q_e to be such that ${q_e}^{-1} = q^{-1} - (R\cos\theta_B)^{-1}$ and note that $p_e^{-1} + q_e^{-1} = p^{-1} + q^{-1}$. The amplitude distribution at the distance q is obtained by means of the Fresnel diffraction integral

$$D(x;q) = \int_{-\infty}^{\infty} \frac{du}{(i\lambda q)^{1/2}} \exp\left[i\pi\frac{(x-u)^2}{\lambda q}\right] D(u),$$

where $D(u)$ is in the form given by equation (12) and x is a coordinate along an axis perpendicular to Ωq (see Fig. 1). The double integral is simplified by performing the integration over u as

$$\int_{-\infty}^{\infty} du \exp\left\{\frac{i\pi}{\lambda}\left[\frac{Lu^2}{pq} - 2u\left(\frac{v}{p_e} + \frac{x}{q}\right)\right]\right\} = \left(\frac{i\lambda pq}{L}\right)^{1/2} \exp\left[-i\frac{\pi pq}{\lambda L}\left(\frac{v}{p_e} + \frac{x}{q}\right)^2\right],$$

having denoted $L = p + q$; we also define $L_e = p_e + q_e$ and we obtain the general formula

$$D(x;q) = \frac{\exp(i\pi x^2/\lambda L)}{(\lambda L)^{1/2}} \int_{-a}^{a} dv \exp\left[\frac{i\pi}{\lambda}\left(\frac{v^2}{L_e} - \frac{av}{R\cos\theta_B} - \frac{2xvq_e}{qL_e}\right)\right] J_0[Z(a^2 - v^2)^{1/2}] \tag{13}$$

and the simple focusing condition

$$p_e + q_e = \pm\alpha q_0. \tag{14}$$

This novel (to the best of our knowledge) formula is a clear generalization of the focusing condition in the case of a flat crystal, which under the same conditions would be $p + q = \pm\alpha q_0$. The focal distances are thereby

$$q_1 = \frac{R\cos\theta_B(\alpha q_0 - p_e)}{R\cos\theta_B + \alpha q_0 - p_e}, \quad q_2 = \frac{R\cos\theta_B(\alpha q_0 + p_e)}{\alpha q_0 + p_e - R\cos\theta_B}. \tag{15}$$

Since a real focus corresponds to a positive value of q_1 or of q_2, we obtain:

(*a*) no real focus if $\alpha q_0 < \min[p_e, R\cos\theta_B - p_e]$ (note that $0 < p_e < R\cos\theta_B$);

(*b*) one real focus if αq_0 has a value between p_e and $R\cos\theta_B - p_e$; and

(*c*) two real foci if $\alpha q_0 > \max[p_e, R\cos\theta_B - p_e]$.

4.3. Coincidence of dynamical and polychromatic focusing and comparison with the approach by Mocella *et al.* (2004, 2008)

The polychromatic focusing condition (1) can be expressed as $R\cos\theta_B = 2pq/(p-q)$, which implies $p_e = q_e = 2pq/(p+q)$. Equation (13) can then be simplified as follows:

$$D(x;q) = \frac{\exp(i\pi x^2/\lambda L)}{(\lambda L)^{1/2}} \int_{-a}^{a} dv\, J_0[Z(a^2 - v^2)^{1/2}] \times \exp\left[i\pi\frac{v^2 L - 2v(ap - aq + 2px)}{4\lambda pq}\right]. \tag{16}$$

The intensity profile is symmetric with respect to $x = -a(p-q)/2p$. The focusing condition is $4pq = \alpha q_o(p+q)$. There is one real focus at the distance

$$q_1 = \frac{\alpha q_0 p}{4p - \alpha q_0} \simeq \frac{\alpha q_0}{4}, \tag{17}$$

where the last expression is valid for $p \gg q_0$, a condition generally satisfied by synchrotron experimental setups. Note that the crystal curvature is such that $R\cos\theta_B = 2pq_1/(p - q_1) = \alpha q_0 p/(2p - \alpha q_0) \simeq \alpha q_0/2$.

In the approach of Mocella *et al.* (2004, 2008), the illumination on the crystal entrance surface is considered to be incoherent, as a consequence of polychromaticity. There would therefore be no influence of the source-to-crystal distance on the dynamical focusing behaviour. Propagation in the bent crystal is regarded to be the same as in a flat crystal, as if the displacement vector were perpendicular to the diffraction vector, which is true only along the neutral surface. The effect of bending is a phase factor related to the curvature of the exit surface. Using the dynamical focusing condition $q^{-1} - (R\cos\theta_B)^{-1} = q_0^{-1}$, which is the same as in §4.1 with the sign '+' and with $\alpha = 1$, we obtain the focusing condition $2pq(p + q)^{-1} = q_0$ for coincidence of the dynamical and polychromatic focusing. The focus position is then obtained as

$$q_1 = \frac{q_0 p}{2p - q} \simeq \frac{q_0}{2}, \tag{18}$$

which is in strong disagreement with formula (17) of the present formulation. Actually, the assumption of effective incoherence, based on considering the crystal propagator to be nearly independent of λ, is justified for the calculation of the reflected intensity distribution close to the crystal exit surface. This is, however, not the case for the in-vacuum propagation after the crystal.

5. Application to experiments

We have applied the present theoretical framework and in particular equation (16) to analyse in a computational manner a series of experiments performed at the energy-dispersive EXAFS beamline ID24 of the ESRF, using the Si 111 reflection of symmetrically cut polychromators in Laue geometry with crystal thicknesses of 200 or 300 μm and mean photon energies 8.3 and 20.0 keV. The horizontally diffracting crystal was placed in an adjustable bender at a fixed distance p = 29.7 m from a secondary source produced by a horizontally focusing mirror acting on the primary beam. A detector was placed at a variable distance q downstream from the crystal, the crystal curvature being adjusted experimentally to minimize the beam size in order to get the focal spot matching the polychromatic focusing conditions for each value of q. No auxiliary measurement of the crystal curvature was made. The experiment's purpose was to detect a minimum of the adjusted beam size for a value of q corresponding to the polychromatic and dynamical focusing coincidence: following the approach by Mocella *et al.* (see §4.3), this was expected to occur for $q \simeq q_0/2$, as predicted by equation (18). The FWHMs shown in Figs. 2 and 3 were obtained *via* a Gaussian–Lorentzian curve fitting of the signal recorded while scanning the focal spot with a slit of approximately 10 μm aperture. In order to obtain the actual FWHM of the beam one should deconvolve the recorded signal taking into account the intrinsic width of the slit. The initial goal of the experiment could not be met since, for each combination of the photon energy and the crystal thickness, a continuous decrease of the measured beam size was detected for q decreasing from about 1500 to 600 or 700 mm (see Figs. 2 and 3). Further reduction of q was not possible due to the mechanical constraints of the beamline setup. In the following, we interpret the experimental results within the present theoretical framework.

Let us first consider the experiment at 20 keV. For the 200 μm thick crystal (Fig. 2), the experimental findings show that the minimum spot size is found at a distance of less than 600 mm, *i.e.* a trend which appears to be in qualitative agreement with the calculations predicting a distance of 500 mm (*cf.* Fig. 4 and Table 1). For the 300 μm crystal, the calculations (Fig. 5) predict a distance of 820 mm, which is inside the experimental range, so that the minimum should have been observed. The failure to detect the minimum can be explained by an additional random deformation of the perfect bent crystal due to internal stresses induced by the bending

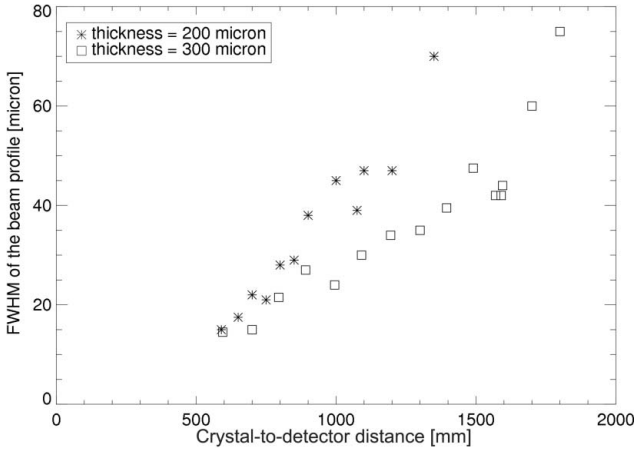

Figure 2
Beam-size measurements for bent Si 111 crystals of two different thicknesses and a polychromatic beam of mean energy 20.0 keV, p = 29 700 mm.

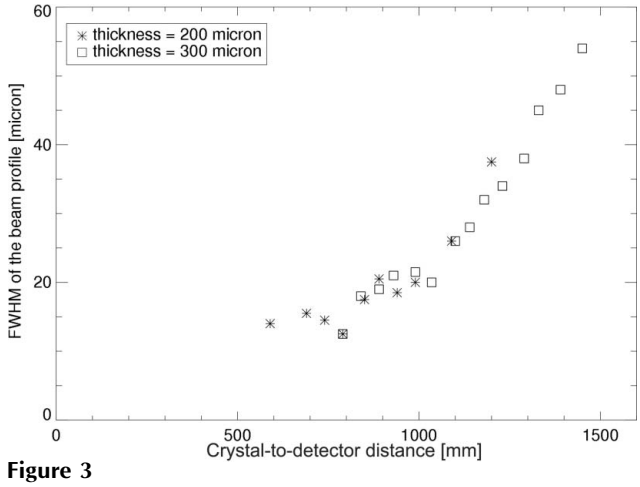

Figure 3
Beam-size measurements for a bent Si 111 crystal and a polychromatic beam of mean energy 8.3 keV, p = 29 700 mm.

Table 1
Experimental results and computational results carried out according to equation (16).

There are no values of $(\alpha q_0/4)_{\rm calc}$ for the 8.3 keV experiments (the reader is referred to the explanation in the text). The numerical results are shown in Figs. 4, 5 and 6.

X-ray energy (keV)	Crystal thickness (μm)	$(\alpha q_0/4)_{\rm exp}$ (mm)	q_0 (mm)	$(\alpha q_0/4)_{\rm calc}$ (mm)
20.0	300	≤600	4500	820
20.0	200	≤600	3000	500
8.3	300	≤800	4300	
8.3	200	≤600	2900	

action and by the heat load; this may result in random fluctuations in the wavefront converging from the crystal to the focus and consequently cause a focus broadening which would increase with the distance q. This is likely to produce a shift of the minimum spot size towards smaller q values; it can also explain the fact that the measured minimum spot sizes are about twice as large as those predicted by the calculations shown in Figs. 4 and 5. It should be mentioned that the energy-dependent numerical values of the crystal susceptibility used in the calculations were taken from the database of optical constants included in the software package *XOP* (Sanchez del Rio, 2011).

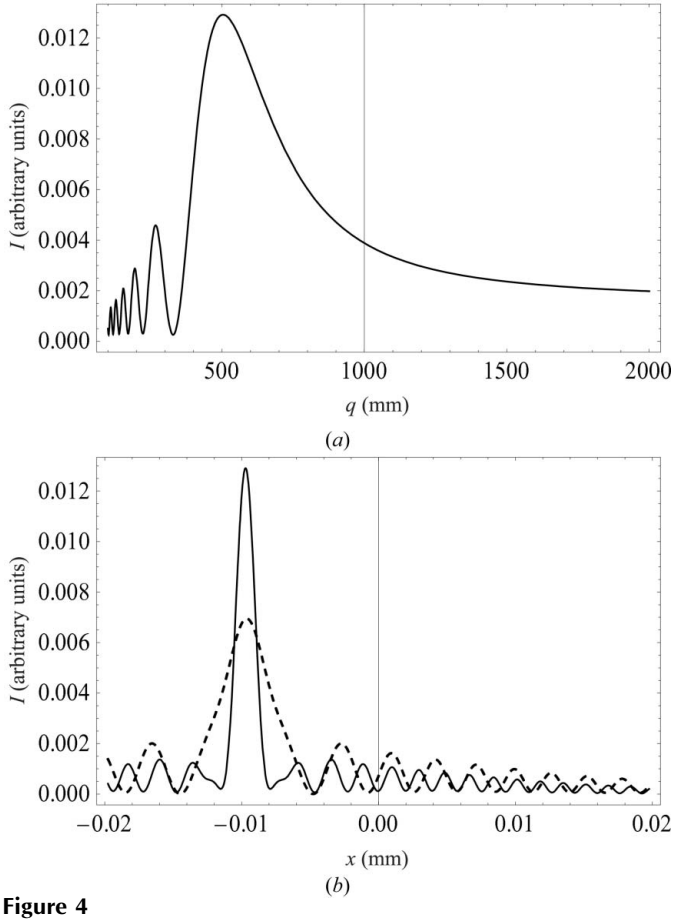

Figure 4
Calculated intensity curves for a bent Si 111 crystal, energy = 20 keV, crystal thickness = 200 μm, p = 29 700 mm, $\theta_{\rm B} = 5.67^\circ$, $\chi_h\chi_{\bar{h}} = 1.684 \times 10^{-12} + i\,1.666 \times 10^{-14}$, q_0 = 2997 mm. (*a*) Intensity at the symmetry centre *versus* q showing the intensity maximum at q = 500 mm, (*b*) intensity profiles for q = 500 mm (solid curve) and for $q = q_0/4$ = 750 mm (dashed curve). Note that α = 0.67.

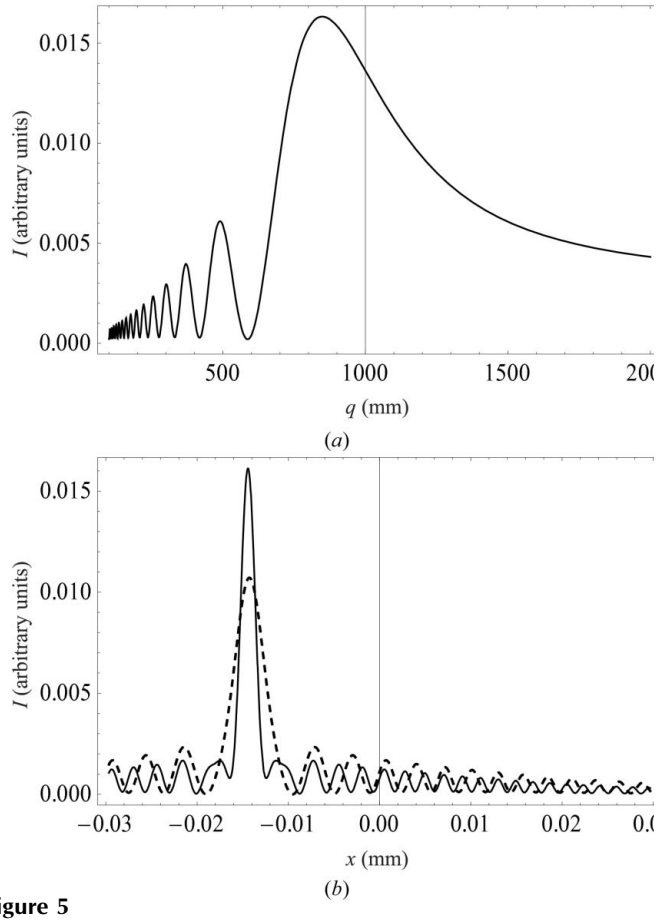

Figure 5
Calculated intensity curves for a bent Si 111 crystal, energy = 20 keV, crystal thickness = 300 μm, q_0 = 4500 mm, the remaining parameters are the same as for Fig. 4. (*a*) Intensity at the symmetry centre *versus* q showing the intensity maximum at q = 820 mm, (*b*) intensity profiles for q = 820 mm (solid curve) and for $q = q_0/4$ = 1125 mm (dashed curve). Note that α = 0.73.

There is apparently no significant spot broadening effect associated with the polychromatic focusing process: the width of the beam hitting the crystal is several millimetres, so the crystal acts as a polychromator diffracting an energy band as large as about 1000 eV; when a narrow slit placed close to the crystal in order to select a limited energy band is moved across the incident beam, the recorded focal spots do not show any significant lateral displacement; this shows that the bending device allows one to approach the following ideal conditions for polychromatic focusing in symmetric Laue geometry: a focusing bent crystal in the form of a hyperbola with the source at one of its foci (Hrdy, 1990).

For an energy of 8.3 keV, the calculated intensities at the symmetry centre show a peculiar behaviour as a function of q (Fig. 6) when compared to the calculations for the 20.0 keV measurements (Figs. 4*a* and 5*a*). The related lateral beam profiles are rapidly oscillating and also differ significantly from the corresponding profiles at 20 keV. This is related to anomalous absorption, as discussed in §2. The interference of

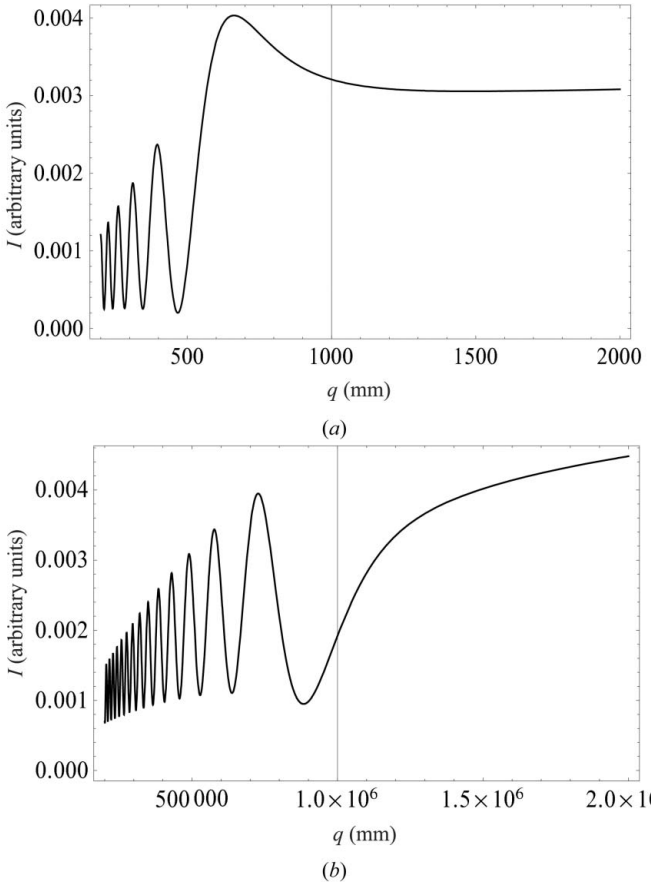

Figure 6
Calculated intensity at the symmetry centre *versus* q for a bent Si 111 crystal, energy 8.3 keV, p = 29 700 mm, $\theta_B = 13.73^\circ$, $\chi_h\chi_{\bar{h}} = 5.781 \times 10^{-11} + i\,3.260 \times 10^{-12}$. (*a*) Crystal thickness = 200 µm, (*b*) crystal thickness = 300 µm.

the convergent and divergent wave components is a minor effect at 20 keV, because the spreading out of the divergent component causes its amplitude to be much smaller than that of the convergent component in the focal region; at 8.3 keV, the amplitude of the divergent component is enhanced with respect to that of the convergent one, as a result of anomalous absorption, and their interference effect becomes significant, in spite of the spreading out of the divergent component.

6. Concluding remarks

The present approach to focusing *via* a bent crystal in symmetric Laue geometry is mainly analytical, in contrast *e.g.* to the approach of Nesterets & Wilkins (2008), which is based on a numerical solution of the TTEs.

Equation (4), which results directly from the spherical-wave theory (Kato, 1961), allows one to explain in a very simple way the dynamical focusing effect and the influence of anomalous absorption on it. It is shown that the bent crystal propagator is not space-invariant and a new formulation of the dynamical focusing is given in terms of only two quantities, which are the effective focal distance of the flat crystal case and $R\cos\theta_B$, which is the product of the radius of curvature and the cosine of the Bragg angle. This novel formulation is applied to the case in which dynamical and polychromatic focusing coincide and provides a comprehensive interpretation of the experimental results, ensuring a far better agreement compared to former computational approaches.

In a future study we intend to propose a generalization of the present theoretical approach to the case of asymmetric crystal reflections, involving the use of confluent hypergeometric functions as the solutions of the TTEs (Petrashen', 1974; Chukhovskii & Petrashen', 1977).

We are greatly indebted to the referees for their comments. Following their recommendations, we have stressed which results are novel compared to the existing literature on this subject.

References

Afanasev, A. M. & Kohn, V. G. (1977). *Fiz. Tverd. Tela*, **19**, 1775.
Aristov, V. V., Polovinkina, V. I., Afanas'ev, A. M. & Kohn, V. G. (1980). *Acta Cryst.* A**36**, 1002–1013.
Aristov, V. V., Polovinkina, V. I., Shmytko, I. M. & Shulakov, E. V. (1978). *JETP Lett.* **28**, 4–7.
Authier, A. (2005). *Dynamical Theory of X-ray Diffraction*, 3rd ed. IUCr Monographs on Crystallography. Oxford University Press.
Chukhovskii, F. N. & Krisch, M. (1992). *J. Appl. Cryst.* **25**, 211–213.
Chukhovskii, F. N. & Petrashen', P. V. (1977). *Acta Cryst.* A**33**, 311–319.
Goodman, J. W. (1968). *Introduction to Fourier Optics*. San Francisco: McGraw-Hill.
Hagelstein, M., Ferrero, C., Hatje, U., Ressler, T. & Metz, W. (1995). *J. Synchrotron Rad.* **2**, 174–180.
Hrdy, J. (1990). *Czech. J. Phys.* **40**, 1086–1089.
Kato, N. (1961). *Acta Cryst.* **14**, 526–532.
Kohn, V. G., Snigireva, I. & Snigirev, A. (2000). *Phys. Status Solidi B*, **222**, 407–423.
Kushnir, V. I. & Suvorov, E. V. (1982). *Phys. Status Solidi A*, **69**, 483–490.
Mocella, V., Ferrero, C., Hrdý, J., Wright, J., Pascarelli, S. & Hoszowska, J. (2008). *J. Appl. Cryst.* **41**, 695–700.
Mocella, V., Guigay, J. P., Hrdý, J., Ferrero, C. & Hoszowska, J. (2004). *J. Appl. Cryst.* **37**, 941–946.
Nesterets, Y. I. & Wilkins, S. W. (2008). *J. Appl. Cryst.* **41**, 237–248.
Petrashen', P. V. (1974). *Sov. Phys. Solid State*, **15**, 2096–2097.
Pinsker, Z. G. (1978). *Dynamical Scattering of X-rays in Crystals*. Springer Series in Solid-State Sciences. Berlin: Springer Verlag.
Sanchez del Rio, M. (2011). *Proc. SPIE*, **8141**, 814115.
Sanchez del Rio, M., Ferrero, C., Chen, G.-J. & Cerrina, F. (1994). *Nucl. Instrum. Methods Phys. Res. A*, **347**, 338–343.
Takagi, S. (1962). *Acta Cryst.* **15**, 1311–1312.
Takagi, S. (1969). *J. Phys. Soc. Jpn*, **26**, 1239–1253.
Taupin, D. (1964). *Bull. Soc. Fr. Mineral. Cristallogr.* **87**, 69.
Taupin, D. (1967). *Acta Cryst.* **23**, 25–35.